Transcription Inhibition of Oncogenic *KRAS* by a Mutation-Selective Peptide Nucleic Acid Conjugated to the PKKKRKV Nuclear Localization Signal Peptide†

S. Cogoi,‡ A. Codognotto,‡ V. Rapozzi,‡ N. Meeuwenoord,§ G. van der Marel,§ and L. E. Xodo*,‡

Department of Biochemical Science and Technology, School of Medicine, University of Udine, P. le Kolbe 4, 33100 Udine, Italy, and Gorlaeus Laboratories, University of Leiden, 2300 RA Leiden, The Netherlands

Received March 22, 2005; Revised Manuscript Received May 27, 2005

ABSTRACT: Mutations in the Kirsten ras (*KRAS*) gene are present in almost all pancreatic adenocarcinomas, and one common mutation is at codon 12: GGT (Gly) is transformed into GAT (Asp). In this work we have targeted the *KRAS* coding sequence embracing the GAT mutation with a sense PNA molecule (**P14**), with the aim of downregulating the expression of the mutant allele. **P14** was designed with a 15-base sequence complementary to the antisense strand of *KRAS* at the GAT (Asp) mutation and conjugated to the nuclear localization signal peptide PKKKRKV. CD spectra as a function of temperature show that **P14** (2 μM) binds to the antisense strand of the GAT target in the mutated allele with a T_M of 78 °C and to the antisense strand of the GGT target in the wild-type allele with a T_M of 69 °C, in 50 mM Tris-HCl, pH 7.4, and 1 M NaCl. Moreover, **P14** showed a high capacity to enter and accumulate in the nuclei of pancreatic cells (Panc-1 and BxPC3), whereas the nonconjugated analogue did not. Quantitative RT-PCR showed that 1 μM **P14** was able to specifically suppress *KRAS* transcription in Panc-1 cells, which harbor mutant *KRAS*, but not in BxPC3 cells, which contain only wild-type *KRAS*. However, **P14** inhibited *KRAS* transcription also in BxPC3 cells when used at concentrations of 5 and 10 μM. Following a single PNA treatment, changes in protein level were evident only in Panc-1 cells. As we found that all three genes of the *ras* family are expressed in the pancreatic cells, we designed PNA−NLS conjugates (**P16** and **P17**) to target also *HRAS* and *NRAS*. The binding of each PNA conjugate to the *ras* genes was assayed by electrophoresis, and their capacity to inhibit transcription was measured by RT-PCR. All of the data obtained, both in vivo and in vitro, are discussed in terms of sequence specificity in the binding between PNA−NLS molecules and genomic DNA.

Pancreatic cancer is one of the most aggressive human cancers that is characterized by a high resistance to currently available treatments (*1*). Like many other malignancies, pancreatic cancer develops because of the accumulation of genetic abnormalities. More than 85% of pancreatic ductal cancers have an activating point mutation in the *KRAS* gene at a very early stage of the cellular transformation (*2*). The *KRAS* human gene is located in chromosome 12, locus 12p12.1, and encodes for a protein of 21 kDa ($p21^{Ras}$) which is associated to the plasma membrane through a prenylation group (*3*, *4*). This protein is active when bound to GTP and inactive when GTP is hydrolyzed to GDP (*5*). Genetic alterations at codons 12, 13, and 61 of *KRAS* impair the capacity of $p21^{Ras}$ to hydrolyze GTP in GDP, with the result that the protein is maintained in the active state while constantly transmitting to the nucleus mitogenic signals (*6*). Other genetic alterations such as *KRAS* amplification and overexpression have been detected in primary pancreatic cancer cells (*7*). In light of these findings, the *KRAS* gene may be an important target for cancer therapy. In previous studies we used aptameric oligonucleotides binding to a critical nuclear protein to suppress the transcription of the *KRAS* gene (*8*, *9*). As carcinoma pancreatic cells are heterozygous for *KRAS*, the aptameric strategy affects both wild-type and mutated *KRAS* alleles. To downregulate primarily the expression of the mutant allele, we investigated a new molecular strategy by using peptide nucleic acid (PNA)[1] to block directly transcription of the mutant *KRAS* allele. PNA is a DNA mimic with a pseudopeptide backbone composed of *N*-(2-aminoethyl)glycine units linked by amide bonds (*10*). The purine (A and G) and the pyrimidine (C and T) heterobases are attached to this polyamide backbone through a methylene carbonyl linkage. PNA is resistant to nucleases and proteases and, being uncharged under physiological conditions, binds to complementary RNA and DNA with high affinity and specificity: the PNA C-terminus corresponds to the 3′ end, while the PNA N-terminus corresponds to the 5′ end (*11*, *12*). An interesting property of PNA is its capacity to invade duplex DNA and form a stable PNA−DNA heteroduplex with the complementary DNA strand (*12*, *13*). Although this process is expected to be kinetically unfavored, the binding of PNA to DNA in the cell is probably less difficult than expected (*14*, *15*). In

† This work has been supported by a grant from the Ministry of Education (PRIN 2003).

* To whom correspondence should be addressed: e-mail, lxodo@makek.dstb.uniud.it; tel, (+39) 0432 494395; fax, (+39) 0432 494301.

‡ University of Udine.

§ University of Leiden.

[1] Abbreviations: NLS, nuclear localization signal; RT, reverse transcriptase; PCR, polymerase chain reaction; CD, circular dichroism; PNA, peptide nucleic acid; T_M, melting temperature.

10.1021/bi0505215 CCC: $30.25
Published on Web 07/14/2005

vivo, the interaction between PNA and the genome is expected to be influenced by DNA supercoiling and the structural changes occurring when chromatin is active. Indeed, the rate with which PNA binds to DNA increases by a few orders of magnitude when the target is negatively supercoiled (*16*) or when chromatin is open and transcriptionally active (*17*). The use of PNA as a therapeutic drug is only possible if the molecule is able to cross the cellular membrane. Initial studies supported the notion that PNA has a very poor intrinsic capacity to penetrate cell membranes, although its backbone is uncharged (*18*). However, a number of recent papers showed that the uptake may vary from cell to cell (*19*−*21*). Previous studies have shown that the uptake can be strongly enhanced by linking the PNA to a bioactive fragment of the nuclear localization signal (NLS) peptide (*22*). The antigene activity of NLS-conjugated PNAs has been convincingly demonstrated by Boffa and co-workers (*22*, *23*). They exposed Burkitt's lymphoma (BL) cells, which harbor a translocated and hyperexpressed c-*myc* oncogene, to an anti-c-*myc* PNA−NLS site-directed against a unique sequence in exon II. They found that the conjugate localized in the nuclei and promoted a rapid downregulation of the c-*myc* gene. Subsequently, the same authors showed that a PNA−NLS conjugate complementary to a specific Eμ intronic sequence blocked the expression of oncogene c-*myc* under Eμ control but not of other c-*myc* alleles (*23*). In this work, we have designed a 15mer PNA molecule fully complementary to *KRAS* codon 12 in the antisense strand of the mutated allele (GAT target) and partially complementary to codon 12 in the wild-type allele (GGT target). This PNA is expected to have a high affinity for the mutated *KRAS* allele and a lower affinity for the wild-type allele. We found that the designed conjugated PNA exhibited a potent antigene activity against *KRAS*, which appeared allele-specific when the PNA was incubated with the cells at the concentration of 1 μM. The designed PNA, **P14**, was found to inhibit *KRAS* transcription in a highly specific manner, as the other members of the *ras* family (*HRAS* and *NRAS*) were not affected. As a parallel objective, we also designed PNA−NLS conjugates for the *HRAS* and *NRAS* genes to evaluate their capacity to specifically inhibit the *ras* genes.

MATERIALS AND METHODS

PNA Synthesis. The PNAs used in this study were made by solid-phase synthesis using a peptide synthesizer (433A; Applied Biosystem, Foster City, CA) and DNA synthesizer (Expedite 8909; PerSeptive Biosystems, Framingham, MA) as previously described (*21*).

Circular Dichroism (CD) Spectroscopy. CD spectra were recorded at various temperatures using a JASCO J-600 spectropolarimeter, equipped with a thermostated cuvette holder and Haake G programmable thermostat. A thermometer inserted in the cuvette holder allowed a precise measurement of the temperature. The spectra were calculated with J-700 Standard Analysis software (Japan Spectroscopic Co., Ltd.) and are reported as molar ellipticity [θ] (deg $\times$ cm^2 $\times$ dmol^{-1}) versus wavelength (nm) [cell length (0.5 cm)], and c is the duplex molar concentration (2×10^{-6}). Each spectrum was recorded three times, smoothed, and subtracted to the baseline. The CD spectra were obtained with PNA−DNA and DNA−DNA solutions (2 μM/duplex) in 50 mM Tris-HCl, pH 7.4, and 1 (or 0.15) mM NaCl, using a 0.5 cm path length cell.

Cell Cultures. Human exocrine pancreas epithelioid carcinoma cells Panc-1 (*24*) and primary adenocarcinoma cells BxPC3 were purchased from the Istituto Zooprofilattico Sperimentale di Brescia (Italy). The cells were cultured in DMEM medium, containing 100 units/mL penicillin, 100 μg/mL streptomycin, 200 mM L-glutamine, and 10% fetal bovine serum (Celbio, Milan, Italy). Cells were maintained in the logarithmic phase of growth, subculturing them twice a week.

Electrophoretic Experiments. Oligonucleotides were labeled by treatment for 1.5 h at 37 °C with T4 polynucleotide kinase in the presence of [γ-^{32}P]ATP. Labeled oligonucleotides were purified by gel filtration chromatography (Sephadex G-50), using water as eluent. Oligonucleotides **1**, **2**, **4**, or **5** (5 nM) were incubated with 25 nM complementary PNA or DNA in 50 mM Tris-HCl, pH 7.4, 150 mM NaCl, and 1 mM EDTA for 2 h at 37 °C. Samples were loaded on a 20% polyacrylamide (acrylamide:bisacrylamide, 19:1) nondenaturing TBE gel and run for 2.5 h at 20 W with temperature control at 25 °C. The gels were fixed in 10% methanol and 10% acetic acid, dried, and exposed to a film for autoradiography. The sequence of **4** (sense *HRAS*) is 5′-ACACCGCCGGCGCCC, while the sequence of **5** (sense *NRAS*) is 5′-ACACCACCTGCTCCA.

Confocal Microscopy. Panc-1 cells were seeded in four-well Falcon culture slides at a density of 5×10^4 cells in 500 μL of DMEM medium supplemented with 10% fetal bovine serum. After 24 h, the cells were exposed for a certain time to fluorescein-labeled PNA and NLS−PNA (**P14**−FITC and **P15**−FITC). The cells were washed twice with PBS and fixed with 3% paraformaldehyde (PFA) in PBS for 20 min. After incubation with 0.1 M glycine containing 0.02% sodium azide in PBS to remove paraformaldehyde and Triton X-100 (0.1% in PBS), the cells were incubated with propidium iodide (6 ng/μL) and RNase A (0.4 μg/mL) for 30 min at 37 °C in order to stain the nuclei. Then cover glasses were mounted on the slides with Mowiol 4-88 and Dabco (2.5%). Cells were analyzed with a Leica DM IRBE confocal imaging system. Diaphragm and fluorescence detection levels were adjusted to reduce to a minimum any interference between fluorescein and propidium iodide channels.

RNA Extraction and RT-PCR Analysis. (A) RNA Extraction. Cellular mRNA was extracted from PNA-treated and untreated cells by Straight A's System reagents kit (Novagen) following manufacturer's protocol. This method is based on the isolation of mRNA with magnetic beads functionalized with oligo(dT).

(B) cDNA Synthesis. mRNA (2.5 μL) were denatured and added to a mix containing (final concentrations) 1× buffer, 0.01 M DTT, 0.8 μM primer dT (dT_{16}; MWG Biotech), 0.2 mM dNTP solution containing equimolar amounts of dATP, dCTP, dGTP, and dTTP (Euroclone), 0.14 unit/μL RNaseOUT ribonuclease inhibitor (Invitrogen), and 4 units/μL M-MuLV reverse transcriptase (BioLabs). The reactions (25 μL per tube) were incubated for 1 h at 37 °C and stopped with heating at 95 °C for 5 min.

(C) Competitor Construction. The competitor was constructed by PCR (see next paragraph) in four steps: (i) a 226 bp fragment from pSV2Cat was amplified; (ii) from the

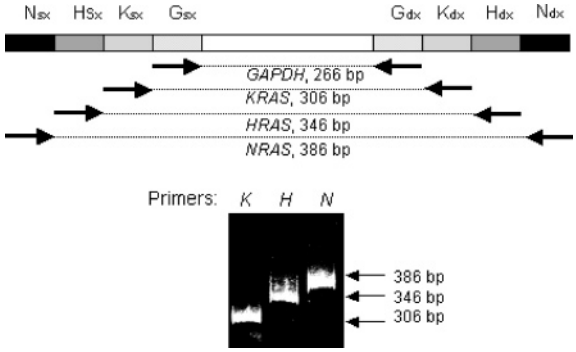

FIGURE 1: Structure of the DNA competitor used to quantify the *RAS* transcripts by quantitative RT-PCR. N, H, and K (sx and dx) are the primer sites for *NRAS*, *HRAS*, and *KRAS* genes, respectively. Gsx and Gdx indicate the primer sites for *GAPDH*. The amplification of the competitor with *KRAS*, *HRAS*, and *NRAS* primers gives DNA fragments of 306, 346, and 386 bp.

226 bp fragment we obtained by PCR a new fragment of 306 bp, adding to the primers the *GAPDH* and *KRAS* sequences; (iii) the 306 bp fragment was elongated to 346 bp with primers containing *KRAS* and *HRAS* sequences; (iv) in the same manner, the 346 bp was elongated to 386 bp using primers containing *HRAS* and *NRAS* sequences so that the termini of this DNA fragment contained *GAPDH*, *KRAS*, *HRAS*, and *NRAS* primer sequences to be used for the amplification. Depending on the set of primers used, the amplification gives rise to 266, 306, 346, or 386 bp fragments using *GAPDH* (Gsx and Gdx), *KRAS* (Ksx and Kdx), *HRAS* (Hsx and Hdx), and *NRAS* (Nsx and Ndx) primers, respectively (Figure 1). Primers were obtained from MWG-Biotech (Florence, Italy): Ksx 5′-GACTGAATATAAACTTGTGG, nucleotides 150−169, and Kdx 5′-TGTTTTGTGTCTACTGTTCT, nucleotides 514−533 (GenBank accession number BC013572); Gsx 5′-AGTATGACAACAGCCTCAAG, nucleotides 476−495, and Gdx 5′-TTTTCTAGACGGCAGGTCAG, nucleotides 793−812 (GenBank accession number M33197); Nsx 5′-TAGATGAATATGATCCCACC, nucleotides 339−358, and Ndx 5′-ATACAACCCTGAGTCCCATC, nucleotides 798−779 (GenBank accession number NM002524); Hsx 5′-TGGACGAATACGACCCCACT, nucleotides 262−281, and Hdx 5′-ACCAACGTGTAGAAGGCATC, nucleotides 737−718 (GenBank accession number BC006499).

(D) Polymerase Chain Reaction (PCR). A volume of 2 μL of cDNA was mixed with the following reagents (final concentrations): 1× Taq buffer with $MgCl_2$, 0.5 mM $MgCl_2$, 1 μM primers, 0.1 mM dTTP, dCTP, dATP, and dGTP (Amersham Pharmacia Biotech), and 0.025 unit/μL EuroTaq DNA polymerase (Euroclone). Amplification was carried out with an automated DNA thermal cycler (Mastercycler personal Eppendorf) as follows: denaturation (94 °C for 30 s), annealing (55 °C for 30 s), and extension (72 °C for 30 s), 25 cycles. *KRAS* amplification was carried out with primers Ksx and Kdx (fragment of 384 bp), *GAPDH* amplification was carried out with primers Gsx and Gdx (fragment of 337 bp), *HRAS* amplification was carried out with primers Hsx and Hdx [fragments of 394 bp, variant 1 (GenBank NM005343), and 476 bp, variant 2], and *NRAS* amplification was carried out with primers Nsx and Ndx (fragment of 460 bp).

Quantification of mRNA was performed as follows. Each RNA sample, extracted from PNA-treated and untreated cells, was converted into cDNA. To a fixed amount of cDNA were added increasing amounts of DNA competitor. The mixtures were amplified using *GAPDH* primers, which provided two distinct bands from cDNA and competitor DNA. The PCR samples were then separated on a 12% polyacrylamide TBE gel. The amount of competitor giving a band of the same intensity as that of *GAPDH* was determined and used for the quantification of the *ras* transcripts. To this purpose, new mixtures containing the same amount of cDNA and a fixed amount of competitor as determined in the previous experiment were co-amplified, but this time with the *KRAS* primers. In this way the levels of *GAPDH* and *RAS* transcripts are normalized against the DNA competitor and can be directly compared. Multiplex PCR was performed without DNA competitor by using in the same reaction tube 0.32 μM *RAS* primers and 0.16 μM *GAPDH* primers. In untreated cells these primer amounts gave *RAS* and *GAPDH* bands of nearly the same intensity.

Western Blots. Western blots were performed according to standard procedures. Western blot analyses were performed on total protein lysates in a 2× Laemmli sample buffer (3.3% SDS, 22% glycerol, 1.1 M Tris-HCl, pH 6, 0.001% bromphenol blue, 10% β-mercaptoethanol). The concentration of the protein lysates was estimated electrophoretically. About 40 μg of each lysate was run in 12% SDS−PAGE and blotted on a nitrocellulose membrane (Shleicher and Shuell) by a Multiphor II Novablot transfer unit (Amersham Pharmacia Biotech). The cellular levels of $p21^{Ras}$, calreticulin, and β-actin were measured using commercially available antibodies. For $p21^{Ras}$ we used as primary antibody a mouse monoclonal antibody specific for p21, used at 3.3 μg/mL (clone 234-4.2; Calbiochem), and as secondary antibody goat anti-mouse IgG (H + L) peroxidase labeled (Euro Clone), used at 0.1 μg/mL. For β-actin we used a commercial actin (Ab-1) kit (Calbiochem) (primary antibody used after a dilution of 1:80000; secondary antibody used at 0.05 μg/mL). For calreticulin we used as primary antibody a rabbit polyclonal antibody (ABR Affinity Bioreagents) diluted 1:5000 and as secondary antibody goat anti-rabbit IgG (H + L) peroxidase labeled (Calbiochem), used at 0.1 μg/mL. Chemiluminescence was detected immediately as described by the manufacturer (Super Signal West Pico; Pierce). Films were exposed for about 15 min for $p21^{Ras}$ and 1 min for β-actin and calreticulin. The intensity of the autoradiography bands was measured with an Ultroscan XL enhanced laser densitometer (LKB Bromma; Pharmacia Biotech).

RESULTS

Structure and Stability of KRAS PNA−DNA Heteroduplexes. Pancreatic carcinoma Panc-1 cells are heterozygous for *KRAS* (25). In these cells the *KRAS* proto-oncogene is mutated at codon 12, whose sequence is changed from GGT (Gly) to GAT (Asp). In the wild-type *KRAS* allele, the sequence encompassing codon 12 is 5′-TGGAGCT**GGT**GGCGTA·5′-TACGCC**ACC**AGCTCCA (GGT target), whereas in the mutated allele the codon 12 sequence changes to 5′-TGGAGCT**GAT**GGCGTA·5′-TACGCC**ATC**AGCTCCA (GAT target), due to a G → A transition. In an attempt to suppress the expression of the mutated *KRAS* allele, we designed a 15mer PNA conjugated to the nuclear localization signal (NLS) PKKKRKV peptide, complementary to the

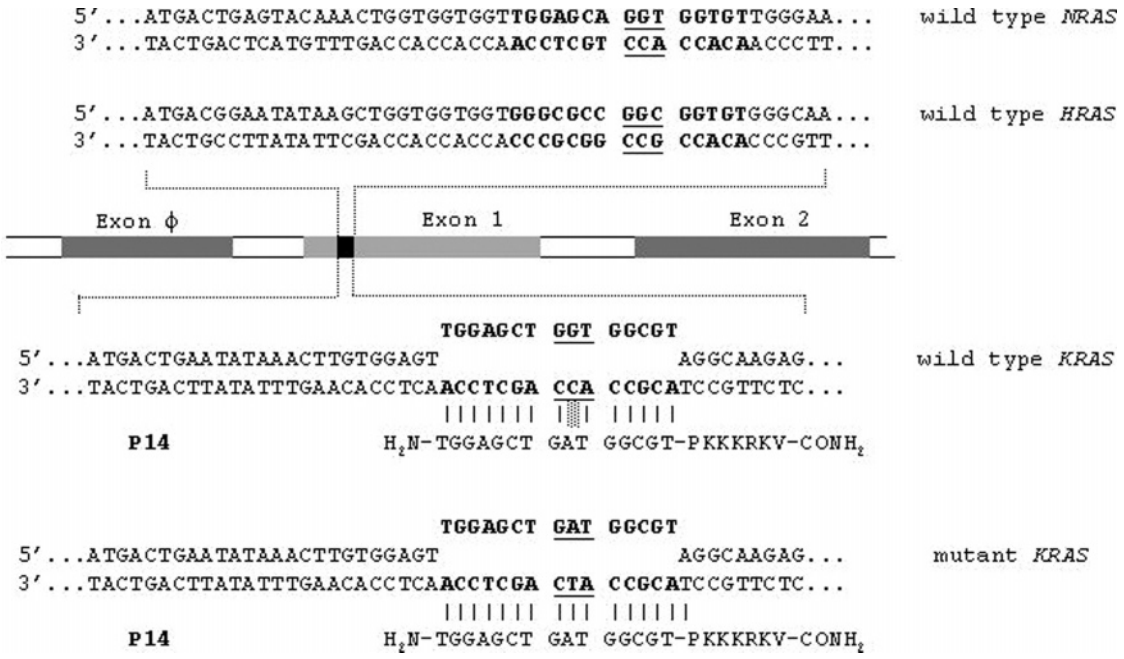

FIGURE 2: Sequences of *KRAS*, *HRAS*, and *NRAS* encompassing codon 12, exon 1. In Panc-1 cells, codon 12 of *KRAS* is mutated: G → A. The sequences of the targets in the wild-type and mutated alleles are shown in bold letters. Codon 12 bases are underlined. P14 is a NLS-conjugated PNA designed to bind to the *KRAS* through a strand displacement mechanism.

Table 1: PNA[a] and DNA Molecules Used in This Study

description	name	PNA−DNA sequence 5′ (N) → 3′ (C)	peptide	modification
sense *KRAS* PNA	**P14**	TGG AGC TGA TGG CGT	PKKKRKV	
scramble PNA	**P31**	GCT AAG GCT ATC GTG	PKKKRKV	
scramble PNA	**P32**	GAT CGG AGT GTG TGC	PKKKRKV	
sense *KRAS* PNA	**P14**−FITC	TGG AGC TGA TGG CGT	PKKKRKV	FL
sense *KRAS* PNA	**P15**−FITC	TGG AGC TGA TGG CGT		FL
sense *HRAS* PNA	**P16**	GGG CGC CGG CGG TGT	PKKKRKV	
sense *NRAS* PNA	**P17**	TGG AGC AGG TGG TGT	PKKKRKV	
wt antisense DNA	**1**	ACG CCA CCA GCT CCA		
mut antisense DNA	**2**	ACG CCA TCA GCT CCA		
mut sense DNA	**3**	TGG AGC TGA TGG CGT		

[a] The structure of the PNA−DNA conjugate (where the linker is a rink amide) is

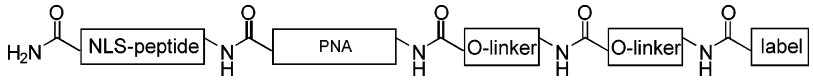

antisense strand of the DNA containing codon 12, nucleotides 174−188 (Gen Bank accession number BC013572) (Figure 2). This conjugate, called **P14**, is expected to form a strong antiparallel PNA−DNA heteroduplex with the GAT target and a weaker heteroduplex with the GGT target located in the wild-type allele, as the latter incorporates a destabilizing A·C mismatched base pair (*11*, *26*−*28*). Previous studies showed that PNA obeys Watson−Crick rules on binding to complementary DNA and RNA strands (*11*). The stability of the PNA−DNA heteroduplexes formed by **P14** was measured by circular dichroism (CD) spectroscopy. As this technique is sensitive to DNA secondary structures, we first compared the spectra of the PNA−DNA hybrids **P14·1** and **P14·2** (see Table 1) with the spectra of the corresponding DNA−DNA duplexes, **1·3** and **2·3** (Figure 3, top). While **1·3** and **2·3** show typical CD spectra of B-form DNA (*11*, *29*), **P14·1** and **P14·2** exhibit spectra different from both B- and A-DNA forms. These spectra, which are similar to that reported for a 15mer PNA−DNA duplex (*11*), are characterized by a strong and positive ellipticity at 264 nm, a weak and negative ellipticity at 240 nm, and a trough near 247 nm. Interestingly, crystal and NMR structures indicate that the PNA−DNA duplexes possess conformational features falling between those of canonical A- and B-form DNA and those of the P-helix (*30*, *31*). Measuring the CD spectra as a function of temperature, we estimated the melting temperature (T_M) of the heteroduplexes (Figure 3, bottom). To minimize possible electrostatic interactions between peptide PKKKRKV and the DNA strand, we performed the melting experiments in 50 mM Tris-HCl, pH 7.4, and 1 M NaCl. Under these conditions, both **P14·2** and **P14·1** displayed a cooperative transition with T_M values of 78 and 69 °C, respectively. In the same buffer, the corresponding DNA−DNA duplexes **2·3** and **1·3** showed T_M values of 75 and 71 °C, respectively. An interesting feature emerging from these data is that both DNA−DNA and PNA−DNA duplexes tolerate an A·C mismatch in the middle of the structure, but while the former is destabilized by only 4 °C, the latter is destabilized by about 8 °C. This finding is in keeping with previous observations that an A·C mismatch is strongly

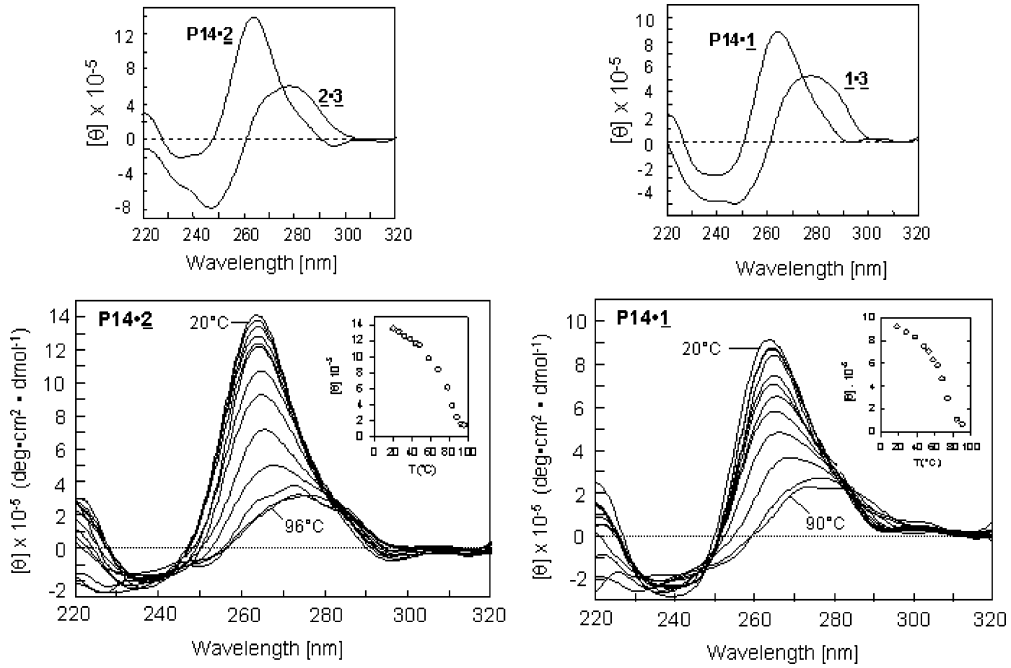

FIGURE 3: (Top) Circular dichroism spectra of PNA−DNA heteroduplexes formed between sense **P14** and antisense DNA strands **1** or **2** encompassing codon 12 in the wild-type and mutated *KRAS* alleles, respectively. The spectra of the analogous DNA−DNA duplexes (**1·3** and **2·3**) are also shown. Spectra have been obtained in 50 mM Tris-HCl, pH 7.4, and 1 M NaCl. The duplex concentration is 2 μM, the cell path length is 0.5 cm. (Bottom) CD spectra **P14·2** and **P14·1** as a function of temperature. The temperatures for the **P14·2** spectra are 20, 26, 32, 38, 44, 48, 58, 68, 78, 83, 88, 93, and 96 °C and for the **P14·1** spectra are 20, 28, 38, 48, 53, 58, 63, 68, 74, 84, and 90 °C. Melting curves provide for **P14·2** a T_M = 78 °C and for **P14·1** a T_M = 69 °C.

destabilizing and can reduce the T_M of a PNA−DNA duplex by up to 20 °C (*11*, *26*, *27*). Under physiological ionic strength conditions (150 mM NaCl), the T_M of **P14·2** and **P14·1** increased to >82 and 71 °C, respectively. Thus, the spectroscopic data indicate that **P14** shows a high affinity for the mutant *KRAS* ATC antisense target DNA strand and a weaker affinity for the wild-type *KRAS* ACC antisense target DNA strand.

PNA−NLS Conjugates Localize in the Nucleus of Panc-1 Cells. Although naked PNA was found to cross the membranes in certain types of cells (*19*, *21*), we found by confocal microscopy that the unconjugated PNA analogue, **P15**−FITC, was completely incapable to enter into Panc-1 cells (Figure 4). We therefore conjugated the C-terminus of the anti-*KRAS* PNA to the nuclear localization signal peptide PKKKRKV (NLS), as previous studies have shown that this covalent modification enables the PNA to enter into the cells and localize in the nuclei (*21*, *22*). We treated, without any transfecting agent, Panc-1 cells for 6 h with 5 μM **P14**−FITC and analyzed the cells by confocal microscopy. As shown in Figure 4, the NLS-conjugated PNA enters into the cells and localizes in both the cytoplasm (green crown surrounding the red nucleus) and the nuclei (yellow color).

Measurements of the Level of KRAS mRNA by Competitive RT-PCR. After having demonstrated that the designed PNA conjugates enter into the nucleus of Panc-1 cells, we assessed whether anti-*KRAS* **P14** produced any biological consequence in the treated cells. First, we measured the level of *KRAS* transcripts in both Panc-1 and BxPC3 cells 13 h following a treatment with 1, 5, and 10 μM **P14** or control PNA, **P31** and **P32** (see Table 1). We used competitive RT-PCR to estimate the effect of the PNAs on transcription. The levels of *KRAS* and *GAPDH* transcripts were estimated relative to a 386 bp DNA competitor, which was appropriately constructed (see Materials and Methods). Total mRNA extracted from PNA-treated and untreated cells was transformed into cDNA, mixed with the DNA competitor, and amplified. The target (cDNA) and competitor shared the same primer recognition sites for both *KRAS* and *GAPDH*. Co-amplification of the target and competitor with the *GAPDH* primers gave DNA fragments of 266 bp from the competitor and 337 bp from cDNA (target), whereas co-amplification with the *KRAS* primers gave DNA fragments of 306 bp (competitor) and 384 bp (target). In each sample we mixed amounts of competitor and cDNA in order to obtain, after amplification with the *GAPDH* primers, two bands of nearly the same intensity. Then, the same mixtures were amplified with the *KRAS* primers. In this way the levels of *KRAS* and *GAPDH* transcripts refer to the same amount of DNA competitor and can be directly compared. Figure 5 shows the results obtained with BxPC3 cells, homozygotic for *KRAS*, and Panc-1 cells that are heterozygotic for *KRAS* but with the mutant allele prevailing over the wild-type allele (*32*). It can be seen that in Panc-1 cells, 13 h following PNA treatment, **P14** strongly suppresses the transcription of *KRAS* but not that of *GAPDH*, at all three concentrations used. A closer inspection of the gel shows that, in the presence of 5 and 10 μM **P14**, the level of *KRAS* mRNA was near to null, while with 1 μM **P14** *KRAS* transcripts were reduced to about 10−20% of the controls (untreated cells and **P31**- and **P32**-treated cells). The same experiment was performed with BxPC3 cells, which are homozygotic for *KRAS* and contain only the weak GGT target. In these cells 1 μM **P14** does not suppress the *KRAS* transcripts, 5 μM **P14** reduces transcription to about 20% of control, and 10 μM **P14** completely suppresses transcription. Since PNA is resistant to nucleases and

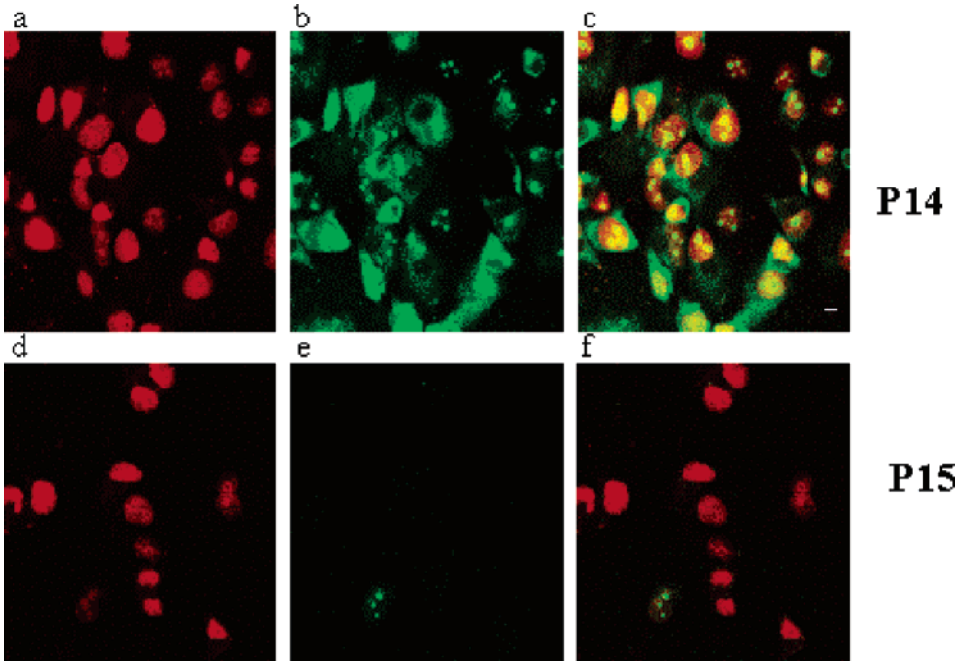

FIGURE 4: Confocal microscopy images of Panc-1 cells treated for 6 h with 5 μM **P14**−FITC and **P15**−FITC. Panels a and d show the nuclei of Panc-1 cells stained with propidium iodide; panels b and e show the green fluorescence emitted by **P14**−FITC and **P15**−FITC; panels c and f show the superimposition of images a−b and d−e. The bar = 5 μm.

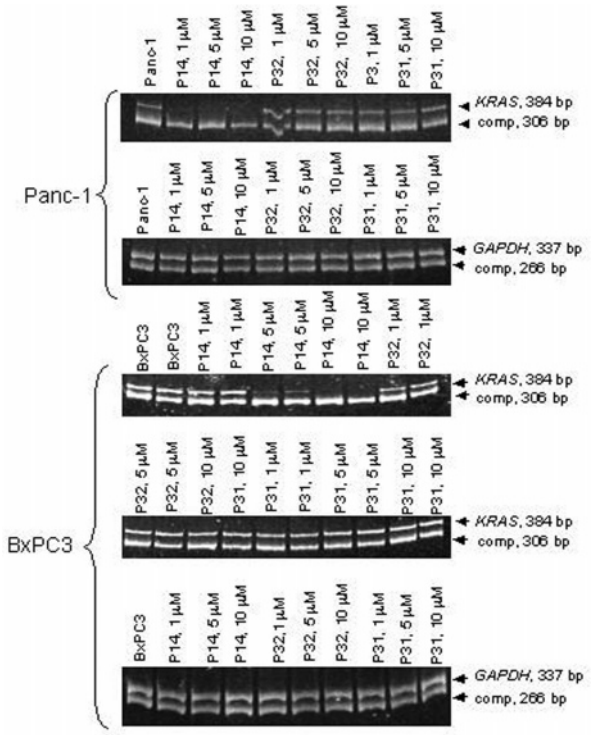

FIGURE 5: Effect of 1, 5, and 10 μM **P14** and control PNA, **P31** and **P32**, on the level of *KRAS* and *GAPDH* transcripts in Panc-1 and BxPC3 cells, determined by competitive RT-PCR, 13 h following PNA treatment. mRNA from treated and untreated cells was extracted, transcribed in cDNA, mixed with a DNA competitor, and amplified. As a control we measured the level of *GAPDH* transcripts, which appears to be the same in both PNA-treated and untreated cells.

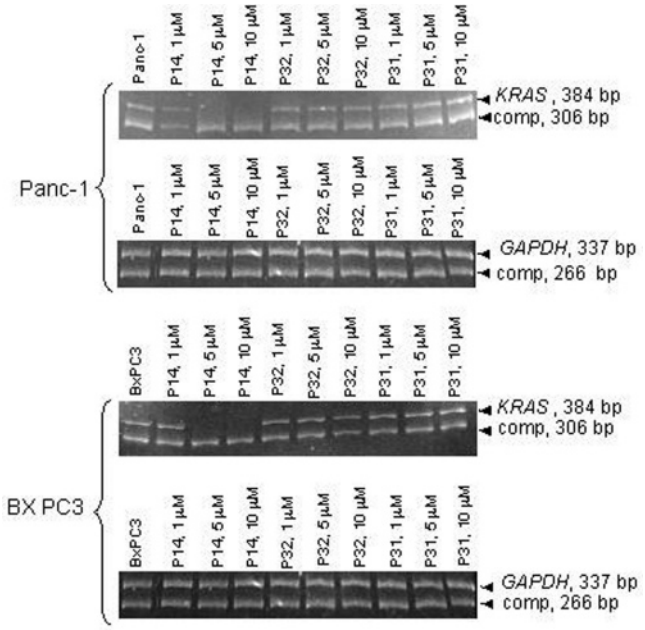

FIGURE 6: Effect on the level of *KRAS* and *GAPDH* transcripts, determined by competitive RT-PCR, in Panc-1 and BxPC3 cells treated for 24 h with 1, 5, and 10 μM **P14** and control PNA (**P31** and **P32**).

proteases, we investigated how long the inhibitory effect lasted in the treated cells. Figure 6 shows that 24 h posttransfection, 1 μM **P14** loses its inhibitory capacity in Panc-1 cells, whereas 5 μM **P14** promoted a partial transcription inhibition in BxPC3 and a total inhibition in Panc-1 cells. This pattern is maintained constant up to 72 h (about one and a half cell divisions). As expected, scramble PNAs, **P31** and **P32**, were always found without any activity against *KRAS* transcription.

Anti-KRAS PNA−NLS Changes the Expression of p21^{Ras} Protein in Panc-1 Cells. As **P14** showed a strong capacity to suppress *KRAS* transcription in Panc-1 cells, we tested whether the level of protein p21^{Ras} changes following a PNA treatment. The half-life of *KRAS* mRNA is only 4 h (*33*), whereas the half-life of p21^{Ras} was estimated to be about 25 h (*34*, *35*). Therefore, we measured the *KRAS* protein at 36 and 55 h after treatment with 5 μM PNA (Figure 7). Either

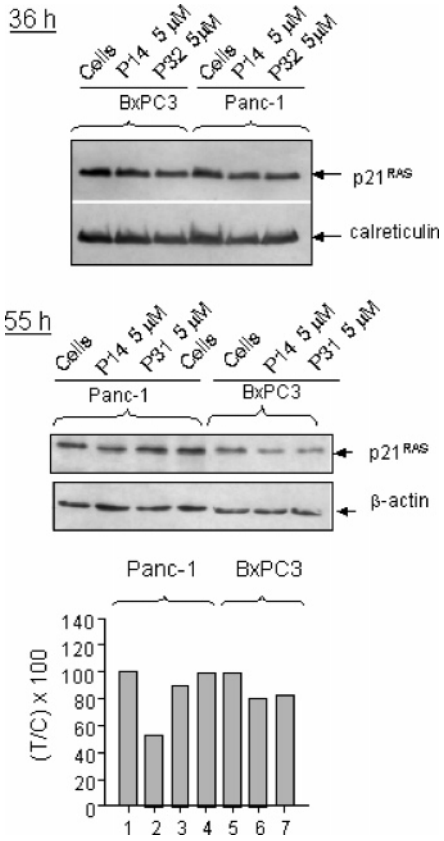

FIGURE 7: Effect of PNA on *KRAS* protein ($p21^{Ras}$) in Panc-1 and BxPC3 cells. Cells were treated with 5 μM PNAs. Total protein extracted from PNA-treated and untreated cells was run in SDS−PAGE and analyzed by Western blot using anti-*KRAS*, anti-β-actin, and anti-calreticulin antibodies. Histograms are relative to the Western blots obtained at 55 h. The ordinate reports the residual $p21^{Ras}/\beta$-actin protein ratio, expressed as % T/C, where T is the $p21^{Ras}/\beta$-actin in PNA-treated cells and C is the $p21^{Ras}/\beta$-actin in PNA-untreated cells.

β-actin or calreticulin was measured as a control for the nonspecific effect on protein synthesis. We did not observe protein level changes at 36 h, neither after a single or a double PNA treatment of Panc-1 and BxPC3 cells. Only at 55 h following PNA treatment did we observe a reduction of the level of *KRAS* protein of 40−50% compared to control, in Panc-1 cells but not in BxPC3 cells. This may be due to the fact that 5 μM **P14** does not completely suppress *KRAS* in BxPC3 cells. Since the half-life of *KRAS* protein is 25 h, 55 h after treatment with **P14** we should have detected a protein residual of about 25% compared to control, and not a value around 50%. The higher protein level is most likely connected to the fact that the commercially available anti-*KRAS* mouse antibody, cKras antibody (234-4.2), cross-reacts with the *HRAS* and *NRAS* proteins, as indicated by the supplier (see Materials and Methods). We then investigated by RT-PCR whether the three *RAS* genes are expressed in Panc-1 and BxPC3 cells. We designed primers for *HRAS* and *NRAS* and found that all three *ras* genes are indeed expressed in Panc-1 and BxPC3 cells to comparable levels. Moreover, it can be seen that **P14** specifically suppresses *KRAS* transcription (Figure 8A). It is therefore likely that the suppression of $p21^{Ras}$ induced by **P14** (40−50% compared to control) is underestimated.

We also investigated by MTT and trypan blue counting the effect of **P14** and **P31** on the viability of Panc-1 and BxPC3. Surprisingly, we observed a little effect on cell viability, although *KRAS* transcription was strongly inhibited by **P14**. Up to 120 h following PNA treatment, roughly corresponding to about three cell divisions, the proliferation of **P14**-treated Panc-1 cells appeared lower by 20−25% compared to untreated cells or cells treated with control **P31** (not shown).

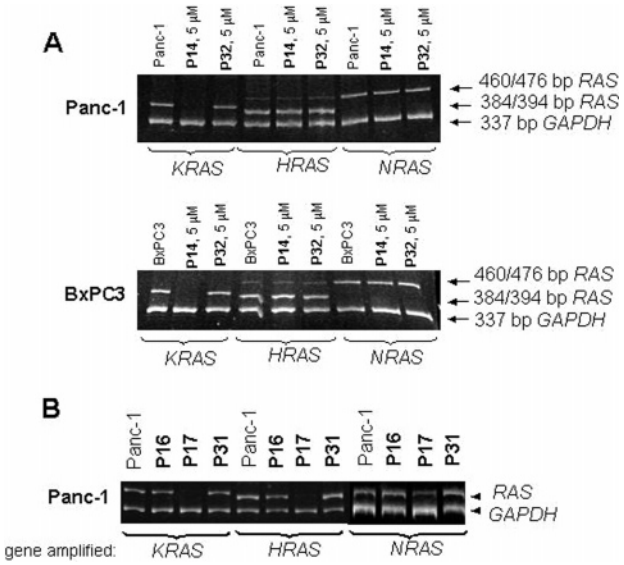

FIGURE 8: (A) Levels of *KRAS*, *HRAS*, and *NRAS* transcripts relative to that of *GAPDH* in Panc-1 and BxPC3 cells treated with **P14** and control **P32**, determined by multiplex RT-PCR. The effect of **P14** on *KRAS* transcription appears to be target specific. (B) Effect of anti-*HRAS* **P16** and anti-*NRAS* **P17** on the transcription of the *RAS* genes. The cells were treated with each PNA conjugate (5 μM). The amounts of the *RAS* transcripts are estimated against *GAPDH* transcripts. Lanes 1−4 (from the left) show the amplification of the *KRAS* gene, lanes 5−8 show the amplification of *HRAS*, and lanes 9−12 show the amplification of *NRAS*.

Target Specificity of PNA−NLS Effector Molecules. The sequences of the *ras* genes at codon 12 are shown in Figure 2. There is sequence homology between targets *KRAS* and *NRAS* (2/3 base changes), but not between *HRAS* and *NRAS* (4/5 base changes) or between *KRAS* and *HRAS* (5 base changes). To investigate whether the *RAS* genes can be individually suppressed, we designed conjugates **P16** and **P17** with a sequence complementary to codon 12 of *HRAS* and *NRAS*, respectively (Table 1). Figure 8B shows the levels of *KRAS*, *HRAS*, *NRAS*, and *GAPDH* transcripts, determined by multiplex RT-PCR, in Panc-1 cells treated respectively with 5 μM **P16**, **P17**, and control **P31**. The results of this experiment combined with those shown in Figure 8A indicate that (i) **P14** recognizes in a sequence-specific manner the *KRAS* target and does not have any effect on the transcription of *HRAS* and *NRAS*, (ii) **P17** inhibits not only the transcription of *NRAS* (its target) but also that of *HRAS* and *KRAS*, and (iii) **P16**, by contrast, does not show inhibitory activity against any of the *RAS* genes. These results were confirmed by competitive RT-PCR (data not shown). To provide a rationale for these data, we analyzed the sequences of the heteroduplexes formed by the designed PNA−NLS conjugates with the *RAS* DNA targets (see Figure 9A). It can be noted that the energy penalty for the binding of **P14** to targets *HRAS* and *NRAS* is high, due to the presence in each duplex of two A·C (C·A) mismatches, which are known to cause a strong duplex destabilization (A·C and C·A destabilize a

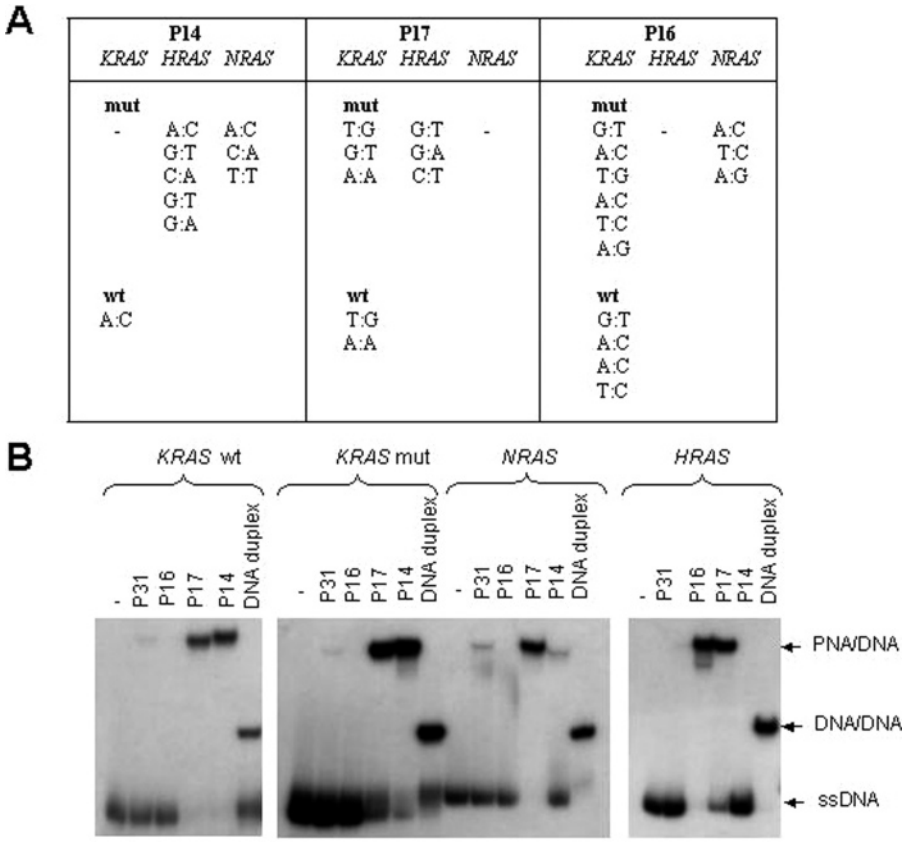

FIGURE 9: (A) Base pair mismatches that should be incorporated in the heteroduplexes formed between **P14**, **P16**, and **P17** and *KRAS*, *HRAS*, and *NRAS* targets. (B) Electrophoretic mobility in 50 mM Tris-HCl (pH 7.4) and 150 mM NaCl of the mixtures containing the *KRAS*, *NRAS*, and *HRAS* targets and the designed NLS-conjugated PNAs. The mixtures were incubated for 2 h at 37 °C and run in a TBE polyacrylamide gel. For comparison, the mobility of the 15mer targets in the double-stranded DNA form are shown.

PNA−DNA duplex by about 20 °C; refs *11*, *26*, and *27* and this work). Conversely, the energy penalty associated to the binding of **P17** to *KRAS* and *HRAS* is expected to be lower, as the corresponding heteroduplexes incorporate mismatches G·T, which induce a lower duplex destabilization (*11*, *26*, *27*). The fact that **P17** inhibits the transcription of all three *RAS* genes indicates that it recognizes the three *ras* targets. Moreover, as **P17** appears to be more efficient against *KRAS* and *HRAS* rather than against its target suggests that codon 12 in the *NRAS* gene should have a scarce accessibility. Finally, for the number and type of mismatches involved, **P16** should bind neither to *KRAS* nor to *NRAS*. Indeed, **P16** did not inhibit transcription of these genes, neither of its own target gene (*HRAS*). A possible explanation for this behavior may be that **P16**, due to its higher G content compared to **P14** and **P17** (60% versus 46.4% and 53.3%), self-associates into unusual structures that are incapable of hybridizing to DNA. Direct experimental evidence supporting the above-mentioned binding and specificity hypotheses was obtained by electrophoresis (Figure 9B). Anti-*RAS* PNA−NLS conjugates were incubated, under physiological conditions, with single-strand *KRAS*, *HRAS*, and *NRAS* DNA targets labeled with ^{32}P and the mixtures run in a polyacrylamide gel. The results show that (i) both wild-type and mutant *KRAS* targets are bound by **P14** and **P17** but not by **P16** or control **P31**, (ii) target *HRAS* is recognized by **P16** and **P17** but not by **P14** or control **P31**, and (iii) target *NRAS* is recognized by **P17** but not by **P14**, **P16**, or control **P31** (a faint band indicating a weak and nonsignificant interaction is observed with **P14** and **P31**). We run for each *RAS* target the corresponding DNA−DNA duplexes that show mobility higher than that of the heteroduplexes. The observation that **P16** binds in vitro to the *HRAS* target, while it does not in vivo (see transcription data), may reflect the different experimental conditions characterizing the two experiments.

DISCUSSION

In this study we have investigated the efficacy of PNA molecules conjugated to the nuclear localization signal peptide to inhibit the transcription of a clinically important gene, the *KRAS* gene, which is mutated in nearly 100% pancreatic (*25*) and 50% colorectal (*36*) adenocarcinomas. Previous molecular approaches to downregulate *KRAS* employed antisense and ribozyme oligonucleotides (*37*−*39*), nucleic acid aptamers (*8*, *9*, *40*), and inhibitors of posttranscription modifications of protein p21^{Ras} (*41*). Although these strategies have given encouraging results, the search for new and more efficient molecules to specifically knock down *KRAS* is of great actuality. The PNA conjugates used in this study behave as antigene molecules and are site-directed against a genome sequence encompassing codon 12, in exon I, of the *KRAS* gene. Pancreatic carcinoma Panc-1 cells are heterozygous for *KRAS* but with the mutant *KRAS* gene prevailing over the wild type. As illustrated in Figure 2, **P14** was designed with a 15mer sequence complementary to the antisense strand of the DNA containing the aspartic point mutation. The binding of **P14** to DNA is expected to occur through a strand displacement mechanism (*42*). In vitro studies showed that this type of binding requires a target duplex not too stable (duplex rich in AT base pairs) and a

low ionic strength (<40 mM NaCl) (*43*). In culture cells, however, the binding of PNA to DNA appeared to be less difficult than expected. This was demonstrated by experiments in which (i) a biotin-labeled PNA that invaded complementary CAG repeats in active chromatin allowed the isolation, using streptavidin−agarose magnetic beads, of transcriptionally active chromatin restriction fragments containing PNA−DNA hybrids (*14*) and (ii) a PNA site-directed against chromosomal targets in fibroblasts promoted a 10-fold increase of the frequency of mutagenesis at the target sequence (*15*). These experiments provide strong, although indirect, evidence that, in vivo, PNA is able to bind to duplex DNA. Under this condition, the binding of PNA to the genome is expected to be kinetically favored by DNA supercoiling and a chromatin opened and transcriptionally active (*16*, *17*, *43*). Another property that antigene PNA should possess is the capacity to penetrate the cell membranes and accumulate in the nuclei. Previous studies have shown that this can be achieved using PNA conjugated to a peptide moiety, of which the most used one is the nuclear localization signal peptide (NLS) PKKKRKV (*21*, *22*, *44*). In this study, we have observed that PNA−NLS conjugates have a high capacity to block the transcription of *KRAS* oncogene expressed in pancreatic adenocarcinomas cells. The inhibitory effect was evaluated by quantitative RT-PCR, for which we constructed a DNA competitor that allows the quantification of the *KRAS* transcript with respect to that of *GAPDH*. We found that the anti-*KRAS* PNA, **P14**, showed a high target specificity, as it binds to its target but not to the *NRAS* and *HRAS* targets, although the sequences of *KRAS* and *NRAS* at codon 12 are very similar. In contrast, the PNA−NLS conjugates designed for the *HRAS* and *NRAS* genes, **P16** and **P17**, exhibited a more complex behavior, as the former did not show any bioactivity, whereas the latter inhibited all three genes of the *ras* family. To provide a rationale for this apparently intriguing behavior, we analyzed by electrophoresis the capacity of the designed PNA−NLS conjugates to hybridize the *RAS* targets. In perfect agreement with the transcription results, we found by electrophoresis that **P14** binds to *KRAS* but not to *NRAS* and *HRAS*, as the interaction with these targets involves the formation of A·C mismatches, which are strongly destabilizing (*11*, *26*−*28*). In contrast, transcription and electrophoretic data show that **P17** binds not only to its *NRAS* target but also to *KRAS* and *HRAS*. This occurs because the interaction of **P17** with the other *RAS* sites involves the formation of G·T mismatches, which are less destabilizing than A·C (*11*, *26*−*28*). Although electrophoretic experiments showed that **P16** binds to its complementary DNA target (*HRAS*), it was found to be incapable of suppressing transcription in Panc-1 cells. It is possible that **P16**, having a high G content (60%), self-associates in unusual structures under physiological conditions (*45*). All of these data suggest that, to design efficient and specific PNA effector molecules, one should take into account that PNA molecules with a high G content (>50%) may self-associate and that G·T mismatches are well tolerated by PNA−DNA heteroduplexes.

Although targeting a point mutation was found to be possible (*46*−*49*), previous attempts to target a *KRAS* point mutation appeared to be difficult (*34*). In contrast, this study shows that **P14** is not only specific for *KRAS* but also discriminates between the wild-type and mutated *KRAS* alleles. Under physiological conditions, 1 μM **P14** suppresses the transcription of the mutated *KRAS* allele but not that of the wild-type allele. This allele specificity appears to be concentration dependent, as it is partially lost at 5 μM and it is completely lost at 10 μM.

Finally, we observed that the transient suppression of *KRAS* transcription did not result in a significant inhibition of cell proliferation. It is noteworthy that, in a previous study conducted on SW80 colorectal adenocarcinoma cells with a homozygous mutation at codon 12 (Gly → Val, GGT → GTT), antisense oligonucleotides designed to target a predicted highly accessible site on the *KRAS* transcript were found to inhibit *KRAS* expression but not cell proliferation (*50*). Moreover, a 20mer antisense phosphorothioate oligonucleotide, ISIS 6957, targeted to the 5′ untranslated region of *KRAS* reduced proliferation in MRC-5 fibroblasts but not in bladder carcinoma T24 cells, although in both cells the *KRAS* transcription was downregulated (*50*). How do we rationalize this apparent incongruence? The three *RAS* genes are expressed in all tissues, albeit to different levels (*32*, *51*). It is, however, not known if the different isoforms are involved in separate signal pathways or if each protein functions similarly and together constitute a functional redundancy within the same *RAS* pathway. The observation that in pancreatic adenocarcinomas Panc-1 cells the suppression of *KRAS* is not enough to inhibit the cell proliferation suggests that in these cells more than one $p21^{Ras}$ isoform could be involved in the *RAS* pathway or that other activated oncogenes predominate in maintaining cell proliferation in these pancreatic cancer cell lines. More work is needed to address this important question.

REFERENCES

1. Bardeesy, N., and DePihno, R. (2002) Pancreatic cancer biology and genetics, *Nat. Rev. 2*, 897−909.
2. Almoguera, C., Shibata, D., Forrester, K., Martin, J., Arnheim, N., and Perucho, M. (1988) Most human carcinomas of the exocrine pancreas contain mutant c-*KRAS* genes, *Cell 53*, 549−554.
3. Goldstein, J. L., and Brown, M. S. (1990) Regulation of the mevalonate pathway, *Nature 343*, 425−430.
4. Kato, K., Cox, A. D., Hisaka, M. M., Grahm, S. M., Buss, J. E., and Der, C. J. (1992) Isoprenoid addition to Ras protein is the critical modification for its membrane association and transforming activity, *Proc. Natl. Acad. Sci. U.S.A. 89*, 6403−6407.
5. Buday, L., and Downward, J. (1993) Epithermal growth factor regulates p21 through the formation of a complex of receptor Grb2 adapter protein and Sos nucleotide exchange factor, *Cell 73*, 611−620.
6. Adjei, A. A. (2001) Blocking oncogenic ras signalling for cancer therapy, *J. Natl. Cancer Inst. 93*, 1062−1074.
7. Yamada, H., Sakamoto, H., Taira, M., Nishimura, S., Shimosato, Y., Terada, M., and Sugimura, T. (1986) Amplifications of both c-Ki-ras with a point mutation and c-myc in a primary pancreatic cancer and its metastatic tumors in lymph nodes, *Jpn. J. Cancer Res. 77*, 370−375.
8. Cogoi, S., Ballico, M., Bonora, G. M., and Xodo, L. E. (2004) Antiproliferative activity of a triplex-forming oligonucleotide recognizing a Ki-ras polypurine/polypyrimidine motif correlates with protein binding, *Cancer Gene Ther. 11*, 465−476.
9. Cogoi, S., Quadrifoglio, F., and Xodo, L. E. (2004) G-rich oligonucleotide inhibits the binding of a nuclear protein to the Ki-ras promoter and strongly reduces cell growth in human carcinoma pancreatic cells, *Biochemistry 43*, 2512−2523.
10. Nielsen, P. E., Egholm, M., Berg, R. H., and Buchardt, O. (1991) Sequence-selective recognition of DNA by strand displacement with a thymine-substituted polyamide, *Science 254*, 1497−1500.
11. Egholm, M., Buchardt, O., Christensen, L., Behrens, C., Freier, S. M., Driver, D. A., Berg, R. H., Kim, S. K., Norden, B., and

Nielsen, P. E. (1993) PNA hybridizes to complementary oligonucleotides obeying the Watson−Crick hydrogen-bonding rules, *Nature 365*, 566−568.
12. Uhlmann, E., Peyman, A., Breipohl, G., and Will, D. W. (1998) PNA: synthetic polyamide nucleic acids with unusual binding properties, *Angew. Chem., Int. Ed. 37*, 2796−2823.
13. Ray, A., and Norden, B. (2000) Peptide nucleic acid (PNA): its medical and biotechnical applications and promise for the future, *FASEB J. 14*, 1041−1060.
14. Boffa, L. C., Carpaneto, E. M., and Allfrey, V. G. (1995) Isolation of active genes containing CAG repeats by DNA strand invasion by a peptide nucleic acid, *Proc. Natl. Acad. Sci. U.S.A. 92*, 1901−1905.
15. Faruqi, A. F., Egholm, M., and Glazer, P. M. (1998) Peptide nucleic acid-targeted mutagenesis of a chromosomal gene in mouse cells, *Proc. Natl. Acad. Sci. U.S.A. 95*, 1398−1403.
16. Bentin, T., and Nielsen, P. E. (1996) Enhanced peptide nucleic acid binding to supercoiled DNA: possible implications for DNA "breathing" dynamics, *Biochemistry 35*, 8863−8869.
17. Boffa, L. C., Carpaneto, E. M., Mariani, M. R., Louissaint, M., and Allfrey, V. G. (1997) Contrasting effects of PNA invasion of the chimeric DMMYC gene on transcription of its myc and PVT domains, *Oncol. Res. 9*, 41−51.
18. Wittung, P., Kajanus, J., Edwards, K., Nielsen, P., Norden, B., and Malmstrom, B. G. (1995) Phospholipid membrane permeability of peptide nucleic acid, *FEBS Lett. 375*, 27−29.
19. Aldrian-Herrada, G., Desarmenien, M. G., Orcel, H., Boissin-Agasse, L., Mery, J., Brugidou, J., and Rabie, A. (1998) A peptide nucleic acid (PNA) is more rapidly internalized in cultured neurons when coupled to a retro-inverso delivery peptide. The antisense activity depresses the target mRNA and protein in magnocellular oxytocin neurons, *Nucleic Acids Res. 26*, 4910−4916.
20. Tyler, B. M., Jansen, K., McCormick, D. J., Douglas, C. L., Boules, M., Stewart, J. A., Zhao, L., Lacy, B., Cusack, B., Fauq, A., and Richelson, E. (1999) Peptide nucleic acids targeted to the neurotensin receptor and administered i.p. cross the blood-brain barrier and specifically reduce gene expression, *Proc. Natl. Acad. Sci. U.S.A. 96*, 7053−7058.
21. Rapozzi, V., Burm, B. E., Cogoi, S., van der Marel, G. A., van Boom, J. H., Quadrifoglio, F., and Xodo, L. E. (2002) Antiproliferative effect in chronic myeloid leukaemia cells by antisense peptide nucleic acids, *Nucleic Acids Res. 30*, 3712−3721.
22. Cutrona, G., Carpaneto, E. M., Ulivi, M., Rondella, S., Landt, O., Ferrarini, M., and Boffa, L. C. (2000) Effects in live cells of a c-myc anti-gene PNA linked to a nuclear localization signal, *Nat. Biotechnol. 18*, 300−303.
23. Cutrona, G., Carpaneto, E. M., Ponzanelli, A., Ulivi, M., Millo, E., Scarfi, S., Roncella, S., Benatti, U., Boffa, L. C., and Ferrarini, M. (2003) Inhibition of the translocated c-myc in Burkitt's lymphoma by a PNA complementary to the Eμ enhancer, *Cancer Res. 63*, 6144−6148.
24. Lieber, M., Mazzetta, J., Nelson-Rees, W., Kaplan, M., and Todaro, G. (1975) Establishment of a continuous tumor-cell line (Panc-1) from human carcinoma from the exocrine pancreas, *Int. J. Cancer 15*, 741−747.
25. Moore, P. S., Sipos, B., Orlandini, S., Sorio, C., Real, F. X., Lemoine, N. R., Gress, T., Bassi, C, Kloppel, G., Kalthoff, H., Ungefroren, H., Loht, M., and Scarpa, A. (2001) Genetic profile of 22 pancreatic carcinoma cell lines. Analysis of *KRAS*, p53, p16 and DPC4/Smad4, *Virchows Arch. 439*, 789−802.
26. Igloi, G. L. (1998) Variability in the stability of DNA-peptide nucleic acid (PNA) single-base mismatched duplexes: real-time hybridization during affinity electrophoresis in PNA-containing gels, *Proc. Natl. Acad. Sci. U.S.A. 95*, 8562−8567.
27. Ratilainen, T., Holmen, A., Tuite, E., Nielsen, P. E., and Norden, B. (2000) Thermodynamics of sequence-specific binding of PNA to DNA, *Biochemistry 39*, 7781−7791.
28. Allawi, H. T., and SantaLucia, J. (1998) Nearest-neighbor thermodynamics of internal A:C mismatches in DNA: sequence dependence and pH effects, *Biochemistry 37*, 9435−9444.
29. Cantor, C., and Schimmel, P. (1980) *Biophysical Chemistry*, Vol. 2, Freeman and Co., San Francisco, CA.
30. Menchise, V., De Simone, G., Tedeschi, T., Corradini, R., Sforza, S., Marchelli, R., Capasso, D., Saviano, M., and Pedone, C. (2003) Insights into peptide nucleic acid (PNA) structural features: The crystal structure of a D-lysine-based chiral PNA-DNA duplex, *Proc. Natl. Acad. Sci. U.S.A. 100*, 12021−12026.
31. Eriksson, M., and Nielsen, P. E. (1996) Solution structure of a peptide nucleic acid-DNA duplex, *Nat. Struct. Biol. 3*, 410−413.
32. Kita, K., Saito, S., Morioka, C. Y., and Watanabe, A. (1999) Growth inhibition of human pancreatic cancer cell lines by antisense oligonucleotides specific to mutated *KRAS* genes, *Int. J. Cancer 80*, 553−558.
33. Chan, S. O., Wong, S. S., and Yeung, D. C. (1992) Transcription induction of c-Ki-ras with the tumour promoter 12-O-tetradecanoylphorbol-13-acetate (TPA) in normal and transformed liver cells, *Mol. Cell. Biochem. 117*, 71−79.
34. Ross, P. J., George, M., Cunningham, D., Di Stefano, F., Jervoise, H., Andreyev, N., Workman, P., and Clarke, P. A. (2001) Inhibition of Kirstein *NRAS* expression in human colorectal cancer using rationally selected Kirstein *NRAS* antisense oligonucleotides, *Mol. Cancer Ther. 1*, 29−41.
35. Lowy, D. R., and Willumsen, B. M. (1993) Function and regulation of ras, *Annu. Rev. Biochem. 62*, 851−891.
36. Meyerhardt, J. A., and Mayer, R. J. (2005) Systemic therapy for colorectal cancer, *N. Engl. J. Med. 352*, 476−487.
37. Andreyev, H. J., Ross, P. J., Cunningham, D., and Clarke, P. A. (2001) Antisense treatment directed against mutated Ki-ras in human colorectal adenocarcinoma, *Gut 48*, 230−237.
38. Kawada, M., Fukazawa, H., Mizuno, S., and Uehara, Y. (1997) Inhibition of anchorage-independent growth of ras-transformed cells on polyHEMA surface by antisense oligodeoxynucleotides directed against *KRAS*, *Biochem. Biophys. Res. Commun. 231*, 735−737.
39. Kijima, H., Yamazaki, H., Nakamura, M., Scanlon, K. J., Osamura, R. Y., and Ueyama, Y. (2004) Ribozyme against mutant *KRAS* mRNA suppresses tumor growth of pancreatic cancer, *Int. J. Oncol. 24*, 559−564.
40. Gilbert, B. A., Sha, M., Wathen, S. T., and Rando, R. R. (1997) RNA aptamers that specifically bind to a K Ras-derived farnesylated peptide, *Bioorg. Med. Chem. 5*, 1115−1122.
41. Prendergast, G. C., and Oliff, A. (2000) Farnesyltransferase inhibitors: antineoplastic properties, mechanisms of action, and clinical prospects, *Semin. Cancer Biol. 10*, 443−452.
42. Demidov, V. V., Yavnilovich, M. V., Belotserkovskii, B. P., Frank-Kamenetskii, M. D., and Nielsen, P. E. (1995) Kinetics and mechanism of polyamide ("peptide") nucleic acid binding to duplex DNA, *Proc. Natl. Acad. Sci. U.S.A. 92*, 2637−2641.
43. Cherny, D. Y., Belotserkovskii, B. P., Frank-Kamenetskii, M. D., Egholm, M., Buchardt, O., Berg, R. H., and Nielsen, P. E. (1993) DNA unwinding upon strand-displacement binding of a thymine-substituted polyamide to double-stranded DNA, *Proc. Natl. Acad. Sci. U.S.A. 90*, 1667−1670.
44. Koppelhus, U., and Nielsen, P. E. (2003) Cellular delivery of peptide nucleic acid (PNA), *Adv. Drug Deliv. Rev. 55*, 267−280.
45. Tackett, A. J., Corey, D. R., and Raney, K. D. (2002) Non-Watson-Crick interactions between PNA and DNA inhibit the ATPase activity of bacteriophage T4 Dda helicase, *Nucleic Acids Res. 30*, 950−957.
46. Woolf, T. M., Melton, D. A., and Jennings, C. G. (1992) Specificity of antisense oligonucleotides in vivo, *Proc. Natl. Acad. Sci. U.S.A. 89*, 7305−7309.
47. Duroux, I., Godard, G., Boidot-Forget, M., Schwab, G., Helene, C., and Saison-Behmoaras, T. (1995) Rational design of point mutation-selective antisense DNA targeted to codon 12 of Haras mRNA in human cells, *Nucleic Acids Res. 23*, 3411−3418.
48. Flanagan, W. M., Kothavale, A., and Wagner, R. W. (1996) Effects of oligonucleotide length, mismatches and mRNA levels on C-5 propyne-modified antisense potency, *Nucleic Acids Res. 24*, 2936−2941.
49. Augustyns, K., Godard, G., Hendrix, C., Van Aerschot, A., Rozenski, J., Saison-Behmoaras, T., and Herdewijn, P. (1993) Hybridization specificity, enzymatic activity and biological (Haras) activity of oligonucleotides containing 2,4-dideoxy-beta-D-erythro-hexopyranosyl nucleosides, *Nucleic Acids Res. 21*, 4670−4676.
50. Chen, G., Oh, S., Monia, B. P., and Stacey, D. W. (1996) Antisense oligonucleotides demonstrate a dominant role of c-Ki-RAS proteins in regulating the proliferation of diploid human fibroblasts, *J. Biol. Chem. 271*, 28259−28265.
51. Bos, J. L. (1989) ras oncogenes in human cancer: a review, *Cancer Res. 49*, 4682−4689.

BI0505215